A Base Station Smart Antenna System for CDMA Cellular

by

Mark C. Roh

S.B. Electrical Engineering and Computer Science
Massachusetts Institute of Technology, 1997

Submitted to the Department of Electrical Engineering and Computer Science

in Partial Fulfillment of the Requirements for the Degree of

Master of Engineering in Electrical Engineering and Computer Science

at the Massachusetts Institute of Technology

June 1998

Author_____
Department of Electrical Engineering and Computer Science
29 May 1998

Certified by_____
Jin Au Kong
Professor of Electrical Engineering
Director, CETA/RLE
Thesis Supervisor

Certified by_____
Eric Yang
Research Scientist, CETA/RLE
Thesis Supervisor

Accepted by_____
Arthur C. Smith
Chairman, Department Committee on Graduate Theses

A Base Station Smart Antenna System for CDMA Cellular

by

Mark C. Roh

Submitted to the
Department of Electrical Engineering and Computer Science

June 1998

in Partial Fulfillment of the Requirements for the Degree of
Master of Engineering in Electrical Engineering and Computer Science

ABSTRACT

Adaptive antenna arrays can increase the capacity of wireless mobile communication systems by reducing cochannel interference. This thesis reviews current base station technology and examines the possibility of implementing an adaptive phased antenna array at a cellular CDMA base station. It is seen that a computationally simple beamforming system and direction-of-arrival estimator can significantly increase system capacity.

Thesis Supervisor: Jin Au Kong
Title: Professor of Electrical Engineering

Thesis Supervisor: Eric Yang
Title: Research Scientist, CETA/RLE

Acknowledgments

I am grateful to:

Roberto Padovani, my QUALCOMM supervisor, who initiated my research and provided valuable guidance during my time with the company.

Ali Tassoudji, who helped me with my initial understanding of antenna arrays.

Rob Gilmore, Debbie Shafer, Lisa Leinhaupel, and everyone else at QUALCOMM who made working there such a pleasure.

Eric Yang, my primary supervisor at MIT, for his time and help with writing and electromagnetic theory.

Prof. Jin Au Kong, who advised me during the early phase of my writing and suggested that I investigate current base station design.

Patrick Kwon, Bernie Chang, Gary Crichlow, and Jennifer Choi, who provided continual encouragement during the writing phase of this project.

My parents, for their love and concern for me. It is to them that my thesis is dedicated.

Finally, I wish to thank God for His faithfulness to me. May all the glory be His.

Contents

Chapter 1

Introduction

The wireless communications industry has experienced phenomenal growth in recent years. Projections indicate that revenues will exceed $100 billion by the year 2000 [5]. With the increase in wireless activity, more efficient methods of using bandwidth are needed.

Adaptive phased antenna arrays offer a solution to the problems of coverage and capacity in cellular communications. Selective beam patterns suppress interference and increase signal-to-noise ratio, resulting in greater system capacity.

The aim of this thesis is to design, develop, and evaluate by computer simulation an antenna array system for use in a CDMA cellular environment.

1.1 Motivation

In a cellular system, a base station (BS) transmits and receives signals from a multitude of cellular phones or mobile units. The BS consists of several antennas which are typically mounted on a tower 100 to 200 feet high in an open area.

The simplest BS architecture is the omnidirectional BS, which transmits and receives signals in all directions. We can increase BS capacity by using directional antennas to

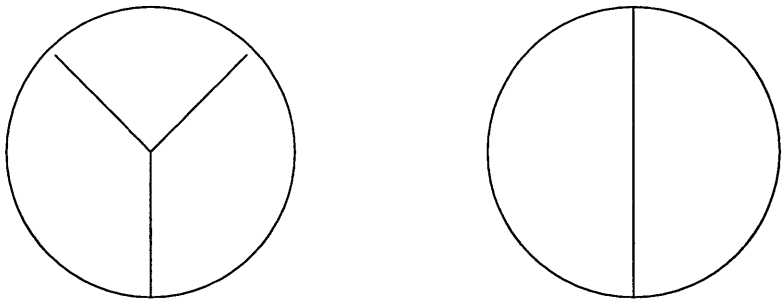

Figure 1.1: A three-sector BS (left) and a two-sector BS.

partition the cell site into multiple sectors [Figure 1.1]. The antennas for each sector suppress signals arriving from other sectors, decreasing interference. Two-sector and three-sector BS designs are commonly used in industry today, increasing capacity by up to a factor of 2.67 when users are uniformly distributed [17].

The generalization of this idea is to incorporate an adaptive antenna array at the base station. Adaptive antenna arrays, or smart antennas, are sets of antennas whose beam pattern adapts with time to maximize some performance metric (e.g., SNR or signal energy). Instead of implementing additional sectors, we form virtual sectors by beamforming. Each user has her own directed beam, and all signals are simultaneously transmitted by the BS. For any given user's beam pattern, many of the interferering signals arrive in the sidelobes of the beam pattern, reducing the interference power.

1.2 Overview of proposed system

Transmitting signals with smart antennas is considerably more difficult than receiving signals, for reasons which will be explained in Section 5.1. We therefore treat in this thesis only the reverse link, in which the BS receives the signals.

We model the received waveforms at the base station as the sum of signals from multiple

users. The waveforms are processed separately for each user; we now describe the decoding process for one particular user. The signals arriving at each antenna are first multiplied by complex weights to suppress interference arriving from other directions. These weights have been previously chosen to form a beam pattern with a single mainlobe and several sidelobes, with the mainlobe centered at the BS's estimate of the direction of arrival (DOA) of the signal. The weighted signals are added together and processed as normal CDMA signals.

The DOA is estimated to be the direction which maximzes total post-CDMA correlated energy. This is reasonable because in CDMA, the received post-correlation signal energy is much greater than the post-correlation interference energy. Therefore, maximizing total energy is equivalent to maximizing the desired signal energy.

This estimate is useful also because it is easy to compute. An optimal metric for adaptive arrays has been determined [10] (cf. Section 5.2), but the necessary computation is prohibitively complex. A simpler estimator was desired for more practical implementation.

The DOAestimator is technically a hypothesis tester. The hypotheses are angles (0°, 10°, 20°, ... 350°) whose beam patterns and weights have been precalculated and stored in BS memory. The system forms a virtual beam for each hypothesis and calculates the returned energy. The DOA estimate is the angle which maximizes total returned energy. The beam pattern associated with this angle is used to filter the received signal, which is then processed in the normal CDMA fashion.

1.3 Document overview

In this thesis we investigate the possibility of using an adaptive antenna array with cellular CDMA, with special attention devoted to a simple proposed system. Chapter 2 reviews the

propagation model for signal transmission and describes various correlation coefficients and their significance for BS design. Chapter 3 considers current BS antenna designs and their radiation patterns, as well as the radiation pattern for the circular array used in the proposed system. Chapter 4 presents an overview of CDMA with an emphasis on issues related to antenna arrays and capacity. Chapter 5 describes recent research in smart antennas and wireless mobile communications. Chapter 6 evaluates of the proposed design. Chapter 7 presents the thesis's conclusions.

Chapter 2

Propagation Model

In this chapter we review the propagation model for wireless mobile communication. We also consider the correlation coefficients of various signals and their consequences for system design.

2.1 Propagation model

For our model of the channel characteristics between BS and mobile, we use the model described in [4]. The model has three main parts: fast fading, shadowing, and path loss.

2.1.1 Fast fading

Figure 2.1 shows the mobile station (MS) and BS in a typical configuration. The MS is surrounded by a circle of local scatterers (buildings) which reflect its signal towards the BS[1]. Since the BS is generally placed in a high and remote location, there are zero scatterers in its locale [7].

If the MS had no scatterers, then the only signal to reach the BS would be the line-

[1]A reasonable estimate of the circle radius is 100 feet, the distance between two buildings.

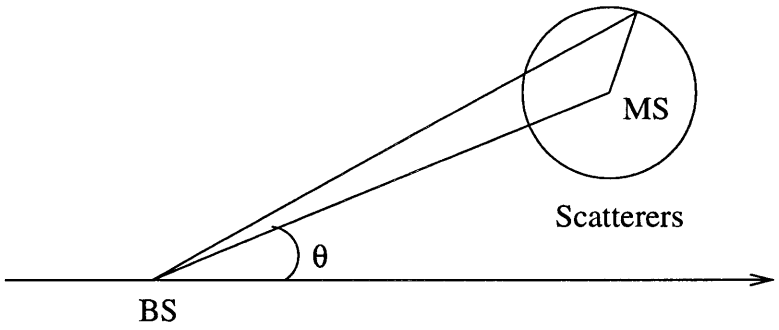

Figure 2.1: Fast fading model.

of-sight signal, and its direction of arrival would be θ. In the presence of scatterers, the arriving wavefronts arrive at a range of angles centered about θ—the beam has "spread." At the BS, these multiple reflected wavefronts interfere constructively and destructively to produce a signal envelope. This envelope, known as fast fading, varies rapidly in magnitude and phase as the mobile moves about. Because fast fading has the Rayleigh probability density, it is also referred to as "Rayleigh fading." In Rayleigh fading, fades of up to 40 dB below the mean level are not uncommon. A simulation of Rayleigh fading is shown in Figure 2.2. In further discussion, we assume fast fading to be flat over the frequency band of interest.

2.1.2 Shadowing

The radio signal is affected by shadowing by hills and buildings, so that the local mean level gradually changes as the mobile moves. Shadowing is a lognormal phenomenon, so that the contribution of shadowing to the overall propagation model is a random variable whose base 10 logarithm behaves as a Gaussian random variable with standard deviation m_d dB. Experimental results have shown that typically m_d varies between 6 and 12 dB; we choose $m_d = 8$ dB for our simulation model.

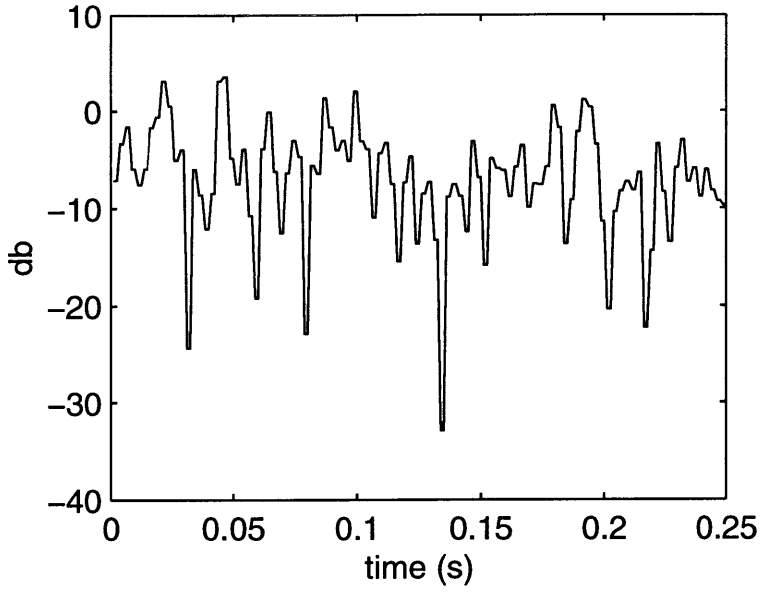

Figure 2.2: Magnitude of fast fading.

2.1.3 Fourth-power law

The path loss obeys a fourth-power law, so that the mean signal power decreases as the fourth power of the distance between base station and mobile.

Thus our propagation model is

$$\text{power loss} = (\text{fast fading}) \times 10^{\zeta/10} \times r^{-4} \tag{2.1}$$

where r is the distance from mobile to BS, and ζ is a zero-mean Gaussian random variable with standard deviation 8.

We note for future reference that shadowing and path loss are independent of transmission frequency, while fast fading varies greatly with frequency.

2.2 Envelope correlation coefficients

2.2.1 Motivation

Adaptive antenna arrays can provide capacity gains in several ways. One method is to spatially filter the signal to reduce interference; this is the approach taken in this paper. Another method is to mitigate Rayleigh fading by exploiting spatial diversity. Rayleigh fading varies with position, and the greater the distance between two points, the smaller the envelope correlation between them. Thus, if two antenna elements are spaced widely enough apart, it is unlikely that both will suffer a deep fade at the same time. Diversity arrays exploit this property by using signal processing techniques to increase the likelihood of recovering the original signal.

In a phased array, if two antenna elements suffer different fading rates, the beam pattern cannot be accurately controlled. Therefore, decorrelation in fading is a hindrance to beamforming systems, even though it benefits diversity systems. The ideal diversity system has antenna elements widely spaced apart, while the beamforming systems require closely spaced elements. The constraints that fast fading places upon array spacing are the topic of Section 2.2.2.

It is also of interest to consider the correlation between Rayleigh fading envelopes on the forward and reverse links of the CDMA system. This is discussed in Section 2.2.3.

2.2.2 Envelope correlation as a function of space

We consider the correlation between the Rayleigh fading envelopes at two MS antennas which receive a signal from a common BS antenna. For an electric dipole linearly polarized

in the $\hat{z}$ direction and suffering fast fading, Jakes [7] gives the cross-covariances as

$$\begin{aligned} E_z: \quad L_e(\tau) &= \frac{\pi}{8} b_0 J_0^2(2\pi f_m \tau) \\ H_x: \quad L_e(\tau) &= \frac{\pi}{8} b_{0H} [J_0(2\pi f_m \tau) + J_2(2\pi f_m \tau)]^2 \\ H_y: \quad L_e(\tau) &= \frac{\pi}{8} b_{0H} [J_0(2\pi f_m \tau) - J_2(2\pi f_m \tau)]^2 \end{aligned}$$

where b_0 and b_{0H} are constants proportional to the energy of the field, f_m is the frequency of the signal, τ is the time interval between measured points, and J_i is the Bessel function of the first kind. Plots of the correlation coefficients vs. $f_m\tau$ are shown in Figure 2.3. (The envelope covariances for (E_z, H_x) and (H_x, H_y) are zero and are not displayed.)

The correlation functions can be interpreted in two ways. First, they can be interpreted as time correlations of the measured fields at a single mobile as it moves about with constant velocity. Second, they can be interpreted as the spatial correlations of the fields at two points in the immediate vicinity of the mobile. If we adopt the second interpretation, then we find that the distance ζ between the two points is related to $f_m\tau$ by $\zeta = \lambda f_m \tau$.

For $\zeta = .5\lambda$, the correlation between elements is quite low. For a cellular system at 900 MHz, an MS moving at 60 miles/hr passes through $.5\lambda$ in less than 5 ms. Thus the Rayleigh envelope changes rapidly as the mobile moves about. This explains the rapidly varying pattern of Figure 2.2.

At the base station, the fading correlation is much less severe. In fact,the correlation is greater than .9 for all antenna separations less than 10λ [7]. We can thus assume a high correlation between antenna elements for our simulation model, so that the beam pattern for phased arrays can be reliably predicted. The asymmetry between BS and MS calculations is a consequence of the assumption that there are no scatterers in the vicinity of the BS.

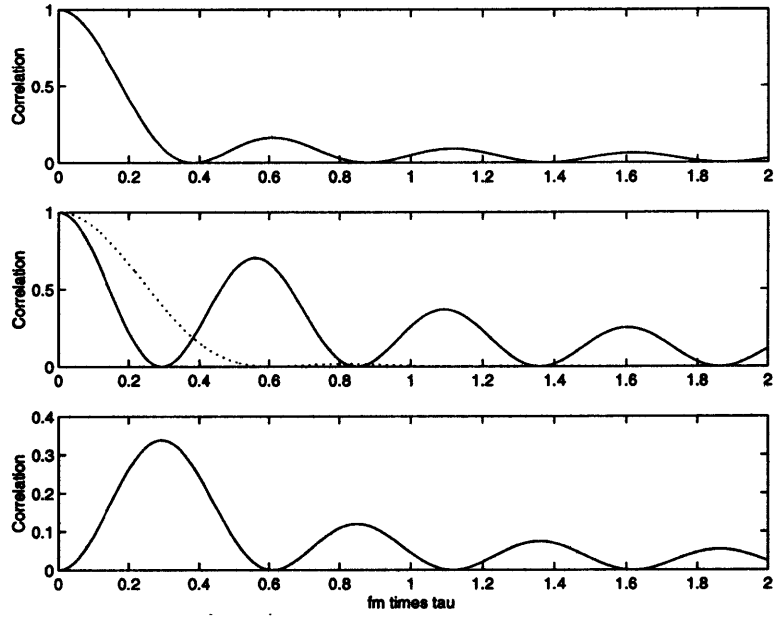

Figure 2.3: Covariance functions of various field envelopes. Top: $|E_z|$. Center dotted: $|H_x|$. Center solid: $|H_y|$. Bottom: Cross-covariance of $|E_z|$ and $|H_y|$.

If there are even a few scatterers scatterers bear the BS, the correlation drops rapidly. We conclude that using beamforming arrays is not practical when the BS is not in a remote location, unless the antenna elements are closed spaced.

2.2.3 Envelope correlation as a function of frequency

Fast fading varies with frequency, and signals at closely spaced frequencies suffer correlated fast fading losses. It is of interest to calculate the envelope correlation coefficient for signals of two different frequencies. This coefficient is

$$\rho_e(s,\tau) \approx \frac{J_o^2(\omega_m \tau)}{1+s^2\sigma^2} \tag{2.2}$$

where s is the frequency separation between the signals, τ is the time separation between the signals, and ω_m is the average of their frequencies [7]. The time delay spread σ is a measure

of the length of time between the arrivals of different multipath elements; σ typically varies around .125 to .75 μsec.

The *channel coherence bandwidth* is defined to be the value of s for which $\rho_e(s, \tau) = .5$. For $\tau = 0$, this yields that $s\sigma = 1$, so that the coherence bandwidth $= 1/2\pi\sigma$. Under reasonable assumptions, the coherence bandwidth for cellular telephony ($f = 836$ MHz) about 640 kHz [7].

In IS-95A[2], the separation between forward and reverse links is 45 MHz. Therefore, the fast fading envelopes are almost completely uncorrelated, and the fast fading envelope of the reverse link is useless as a predictor of the forward link envelope. Therefore, the forward link envelope must be estimated via some other means. In Section 5.1 we will see one such approach.

[2]IS-95A is the current CDMA standard in the United States.

Chapter 3

Base Station Antenna Design

3.1 Overview

Most BS's used today have two or three sectors. A typical sector has three antennas. Two antennas receive reverse link signals and the remaining antenna transmits forward link signals. Some designs employ only two antennas, with one of the reverse link antennas doubling as a transmitting antenna. In either design, signals received at each of the two reverse link antennas are decoded separately.

Two examples of designs used commercially are shown in Figure 3.1; they are taken from the EMS Wireless Product Catalog [3]. The left-hand side shows a system with 12 vertical dipoles in front of an aluminum backplane. The backplane provides shielding from signals arriving from other sectors. The multiple dipoles are oriented in such a way as to transmit and receive maximum power in the horizontal direction or slightly below horizontal (the downtilt can be generated either mechanically or electrically). The right hand side has 12 dipoles against the backplane. Four are vertically polarized, four are oriented in the $+45°$ direction, and four are oriented in the $-45°$ direction. The crossed dipole configuration

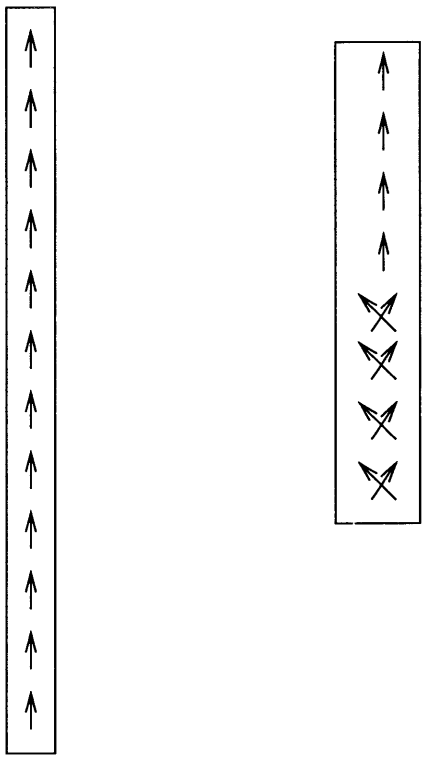

Figure 3.1: Two designs for BS antennas.

exploits polarization diversity, leading to greater capacity [6].

In this chapter we consider BS antenna design. We calculate the radiation pattern of a linear array and consider the radiation pattern of a dipole in front of a reflecting backplane. Finally, the characteristics of the proposed circular antenna array will be analyzed.

3.2 Linear antenna arrays

We calculate the radiation pattern for a linear array, following the analysis in Kong [8]. We consider a linear array with N elements pointing in the $\hat{z}$ direction and spaced along the x axis with equal spacing d [Figure 3.2]. Each element has phase shift α relative to its neighbor. The current density $\bar{J}(\bar{r}')$ is

$$\bar{J}(\bar{r}') = \hat{z} Il \sum_{n=0}^{N-1} e^{in\alpha} \delta(x' - nd)\delta(y')\delta(z') \tag{3.1}$$

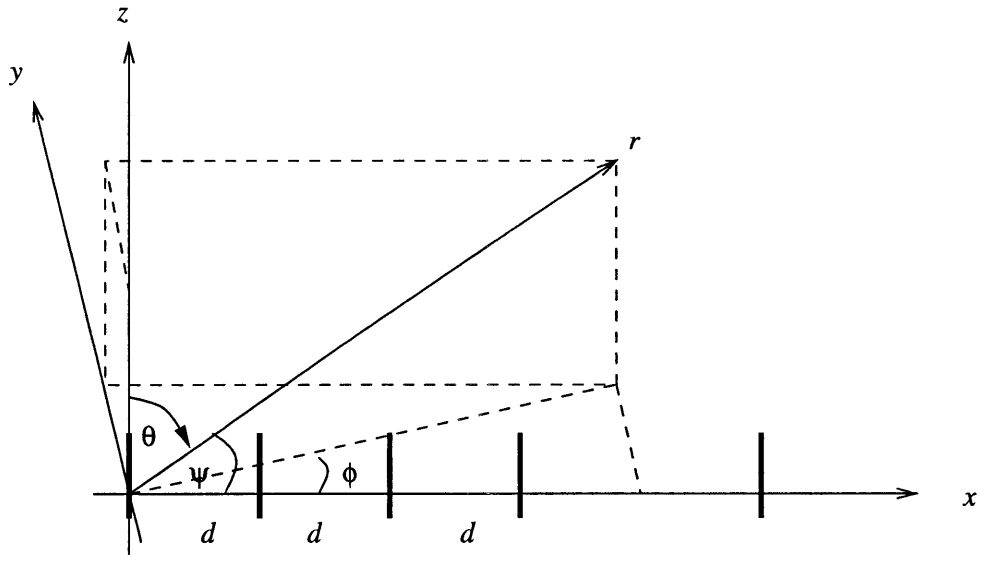

Figure 3.2: Linear antenna array.

The vector current moment is

$$\bar{f}(\theta,\phi) = \int dx' \int dy' \int dz' \bar{J}(\bar{r}') e^{-ik(x' \sin\theta\cos\phi + y' \sin\theta \sin\phi + z'\cos\theta)} \tag{3.2}$$

$$= \int dV' \left[\hat{z} I l \sum_{n=0}^{N-1} e^{in\alpha} \delta(x' - nd)\delta(y')\delta(z') \right] e^{-ik(x' \sin\theta\cos\phi + y' \sin\theta \sin\phi + z'\cos\theta)} \tag{3.3}$$

$$= \hat{z} I l \sum_{n=0}^{N-1} e^{in\alpha} e^{-k(nd \sin\theta\cos\phi)} \tag{3.4}$$

Hence the $\bar{E}$ field in the far field is

$$E_\theta = -i\omega\mu \frac{I l e^{ikr}}{4\pi r} \sin\theta \left[\sum_{n=0}^{N-1} e^{-in(kd\cos\psi - \alpha)} \right] \tag{3.5}$$

where

$$\cos\psi = \sin\theta\cos\phi \tag{3.6}$$

where ψ is the angle between the x axis and $\bar{r}$.

The summation in brackets is called the *array factor.* The expression outside the brackets is the $\bar{E}$ field generated by a single Hertzian dipole. We see then that the antenna pattern for a linear array equals the pattern for a single element times the array factor.

3.3 Dipole antenna with a finite reflector

The EMS antennas cited in Section 3.1 feature an array of dipole antennas with a conducting backplane to provide shielding. In this section we examine the radiation pattern of a single dipole with a backplane.

Figure 3.3 shows the model used. A vertically oriented electric dipole 0 is centered in front of a perfectly conducting backplane. It is well known that the radiation pattern in the $x - y$ plane is nearly independent of the height of the reflector, so that we can assume that

the backplane is infinite in the $\hat{z}$ direction [14]. From the image theorem, we can replace the backplane with a symmetric dipole image 1 with π phase shift from the dipole. This equivalence only holds when P lies inside the boundary surfaces ($\phi' \leq \phi \leq \pi - \phi'$) indicated in the figure; outside the boundary, the image approximation is less accurate because the dominant reflection term does not exist. In this paper we treat only the case where P lies within the boundary surfaces.

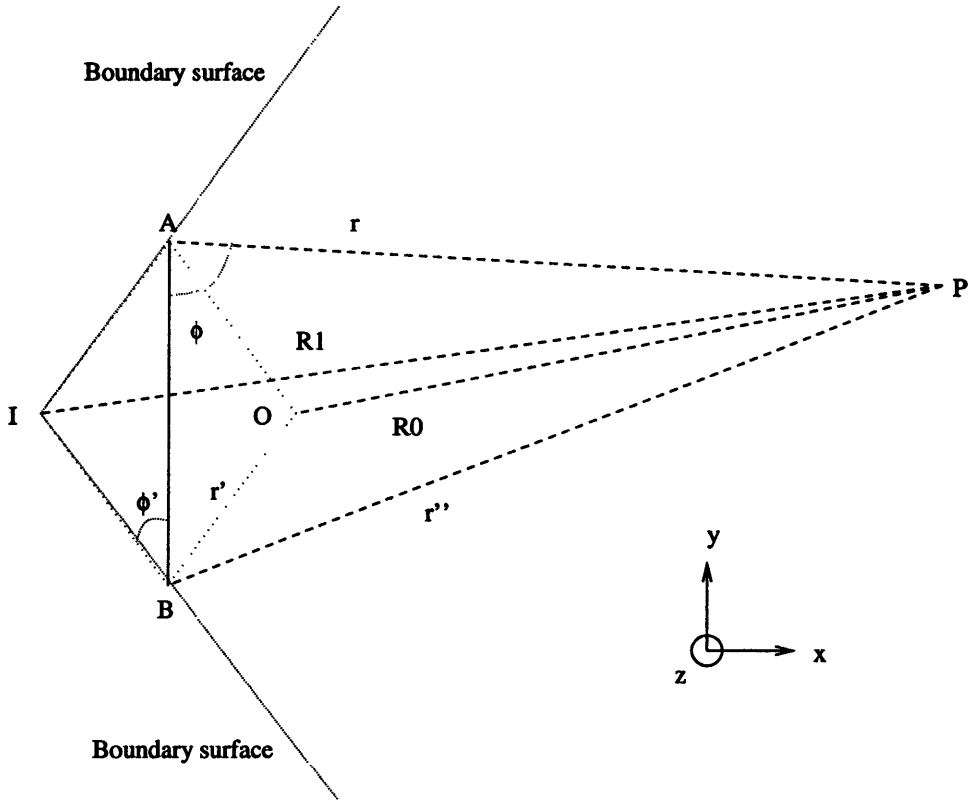

Figure 3.3: Diffraction model.

At the point P, the electric field has six sources: the dipole field I_0, the image field I_1, and the diffracted fields I_{0A}, I_{0B}, I_{1A}, and I_{1B}. We use the Fresnel assumption to calculate the diffracted fields. Let $n = 0, 1$ and $\alpha = A, B$. Nomura [13] (cf. [14]) has treated the case

of a conducting half-plane; we adapt his analysis here to examine the finite-width case.

$$I_n = \frac{e^{ikR_n}}{R_n} \tag{3.7}$$

$$I_{n\alpha} = \frac{e^{ikR_{n\alpha}}}{R_{n\alpha}} f(T_{n\alpha}) \tag{3.8}$$

$$R_0^2 = r'^2 + r^2 - 2rr'\cos(\phi - \phi') + (z - z')^2 \tag{3.9}$$

$$R_1^2 = r'^2 + r^2 - 2rr'\cos(\phi + \phi') + (z - z')^2 \tag{3.10}$$

$$R_{0A}^2 = R_{1A}^2 = (r' + r)^2 + (z - z')^2 \tag{3.11}$$

$$R_{0B}^2 = R_{1B}^2 = (r' + r'')^2 + (z - z')^2 \tag{3.12}$$

$$T_{n\alpha} = k(R_{n\alpha} - R_n) \tag{3.13}$$

$$f(T) = \frac{1}{\sqrt{\pi}} e^{-i(\pi/4 + T^2)} \int_T^\infty e^{it^2} dt = \frac{e^{-iT^2}}{2} X(T) \tag{3.14}$$

$$X(T) = \{1 - C(T) - S(T)\} - i\{S(T) - C(T)\} \tag{3.15}$$

where $C(T)$ and $S(T)$ are the Fresnel integrals

$$C(T) = \int_0^T dt \cos(\pi t^2/2) \tag{3.16}$$

$$S(T) = \int_0^T dt \sin(\pi t^2/2) \tag{3.17}$$

A typical BS antenna design is that of the EMS OptiFill FV105-10-XXXX-2 series, which has a 3 dB azimuth beamwidth of 105°. This is the design shown in the left half of Figure 3.1 consisting of 12 vertical dipoles. The outer dimensions (L × W × D) of the FV105-10-XXXX-2 are 48 in × 12 in × 7 in. This suggests that for a 900 MHz signal, $l = 3.7\lambda$, $w = .92\lambda$, and $d = .54\lambda$. The distance from dipole to backplane is some value less than d. In Figure 3.4, plots of the radiation pattern for a single dipole are shown for $w = .46\lambda$ and various values of d. In this configuration, there is only the dipole and

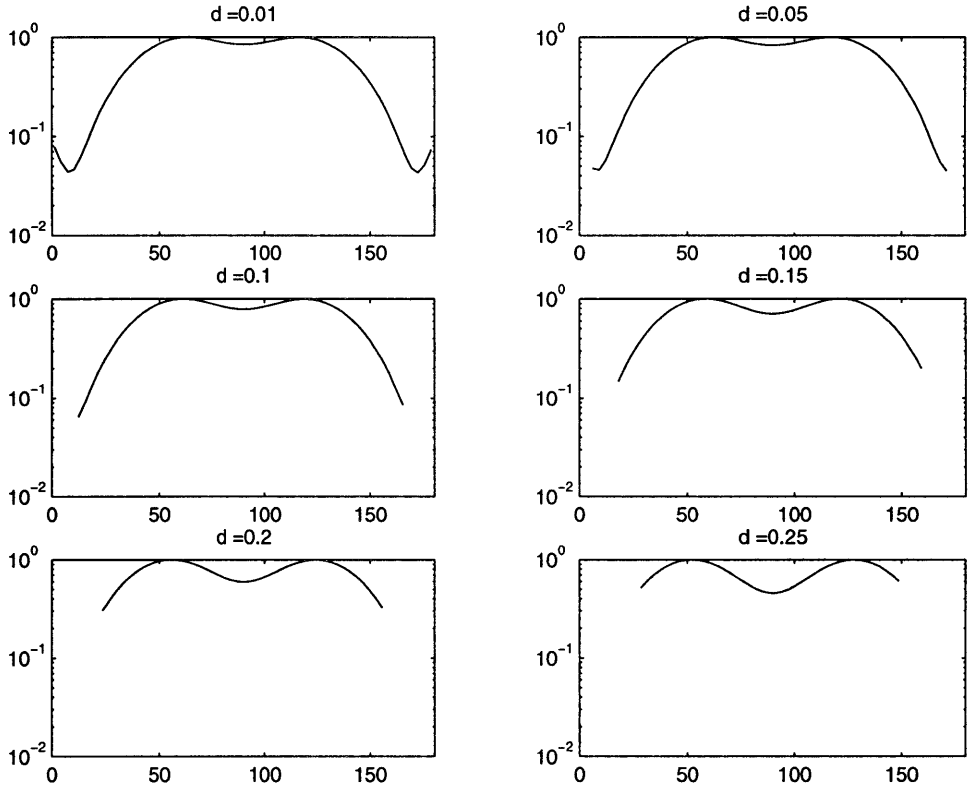

Figure 3.4: Radiation patterns (power vs. angle) for a dipole with back plane reflector; $w = .92\lambda$. The plots are displayed for values of ϕ inside the boundary surfaces.

its image; there is no diffraction. The resulting radiation pattern is shown in Figure 3.5. Finally, in Figure 3.6 we show the beam pattern of the antenna itself, from measured data taken from the EMS Catalog.

It appears that for this configuration, $\phi = 90°$ is a local minimum, with the decrease more pronounced for greater values of d. This phenomenon is a consequence of the diffraction estimation at the edges of the backplane. For $\phi \approx \pi/2$, we expect that the fields from the dipole and its image would be much greater than the diffracted fields, but it is not the case here. This is because the Fresnel approximation is less accurate for large angle values. We do see, however, that the radiation power decreases towards the extreme values of ϕ as expected. We also expect little power to be transmitted in the directions outside the

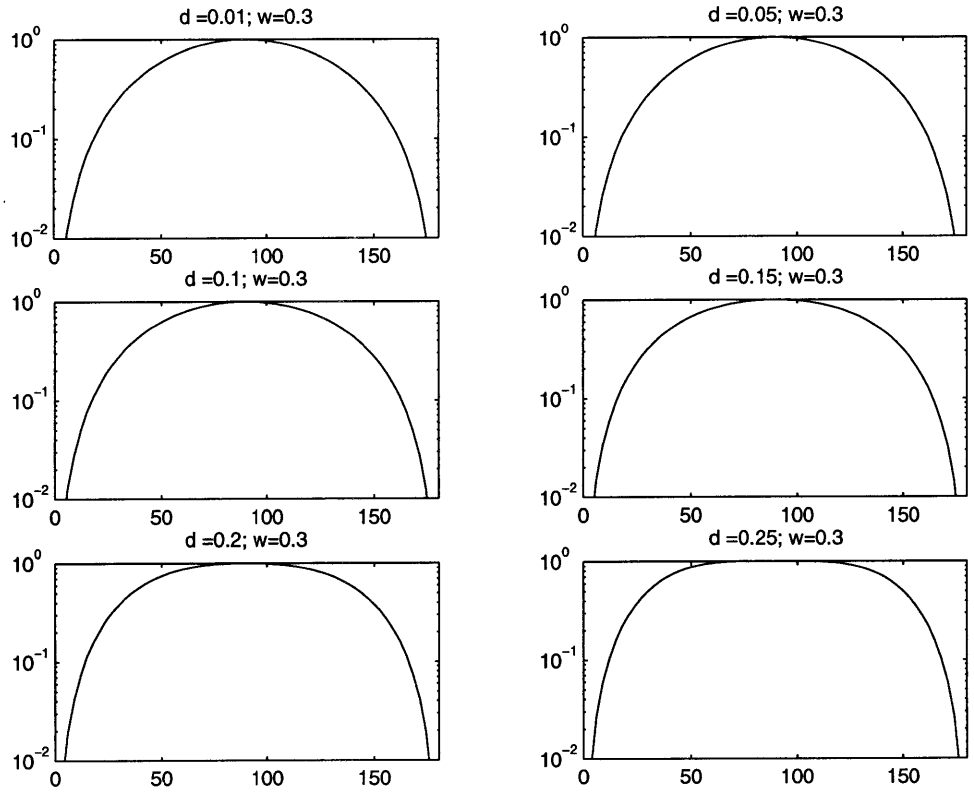

Figure 3.5: Radiation patterns (power vs. angle) for a dipole with an infinte back plane reflector (no diffraction).

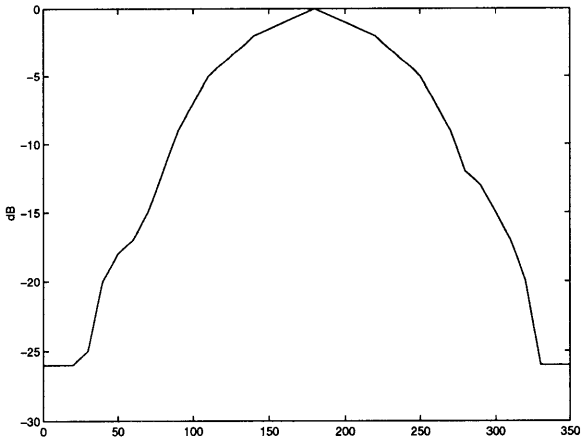

Figure 3.6: Radiation patterns (power vs. angle) for the FV105-10-XXXX-2 BS antenna.

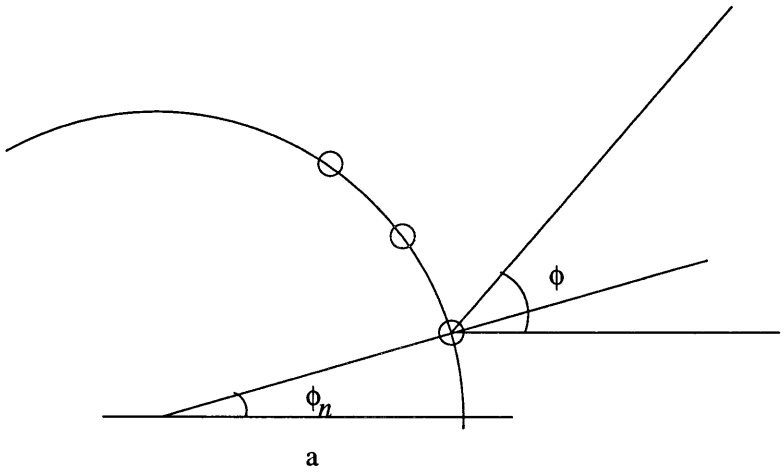

Figure 3.7: Circular array.

boundary surfaces, although the values are not calculated here.

We also see that Figure 3.6 is in good agreement with the plots in Figure 3.5.

3.4 Circular antenna arrays

If the MS and BS are far apart, we can assume that each arriving wavefront is planar (the far-field condition). From Kong [8], the far-field criterion is

$$r > \frac{2D^2}{\lambda} \tag{3.18}$$

where r represents the distance from antenna to field source, D is the aperture width, and λ is the wavelength. For the 800 MHz cellular band, $\lambda \approx 35$ cm; for the 1.9 GHz PCS band, $\lambda \approx 16$ cm. For an antenna array with $D < 2\lambda$, we have that $r > 3$ meters is a sufficient condition to be in the far field.

We choose a circular array because of its symmetry properties. We calculate here the beam pattern of a circular array; a more detailed treatment can be found in [11].

Consider a single-ring array of radius a as shown in Figure 3.7. The ring is in the $x-y$ plane. There are N isotropic elements placed along the circumference. To calculate the far-field array pattern, we add the contribution from each element:

$$E(\phi) = \sum_{n=1}^{N} I_n \exp[jka\cos(\phi - \phi_n) + j\alpha_n] \tag{3.19}$$

where I_n is the current excitation of the nth element located at $\phi = \phi_n$, α_n is the associated phase excitation (relative to the array center), and k is the magnitude of the wave vector. For the conventional *cophasal* array, the phase excitations are chosen so that the beams match phase for the desired direction ϕ_0 of the mainlobe:

$$\alpha_n = -ka\cos(\phi_0 - \phi_n) \tag{3.20}$$

In our implementation, we choose uniform current excitation, so that $I_n = I$, and uniform spacing, so that $\phi_n = 2\pi n/N$. (An array with uniform current excitation is referred to as a *phased array*). For the cophasal array, this yields

$$E(\phi) = I\sum_{n=1}^{N} \exp[jka\cos(\phi - 2\pi n/N) - jka\cos(\phi_0 - \phi_n)] \tag{3.21}$$

We choose $a = \lambda/(4\sin(\pi/N))$ to obtain $\lambda/2$ spacing between adjacent elements. Substituting $k = 2\pi/\lambda$, we obtain

$$E(\phi) = I\sum_{n=1}^{N} \exp[j\frac{\pi}{2\sin(\pi/N)}(\cos(\phi - 2\pi n/N) - \cos(\phi_0 - 2\pi n/N))] \tag{3.22}$$

Figure 3.8 displays plots of the beam pattern ($|E(\phi)|^2$ vs. ϕ) for various values of N. Since we stipulated $\lambda/2$ interelement spacing, the arrays increase in physical size with N.

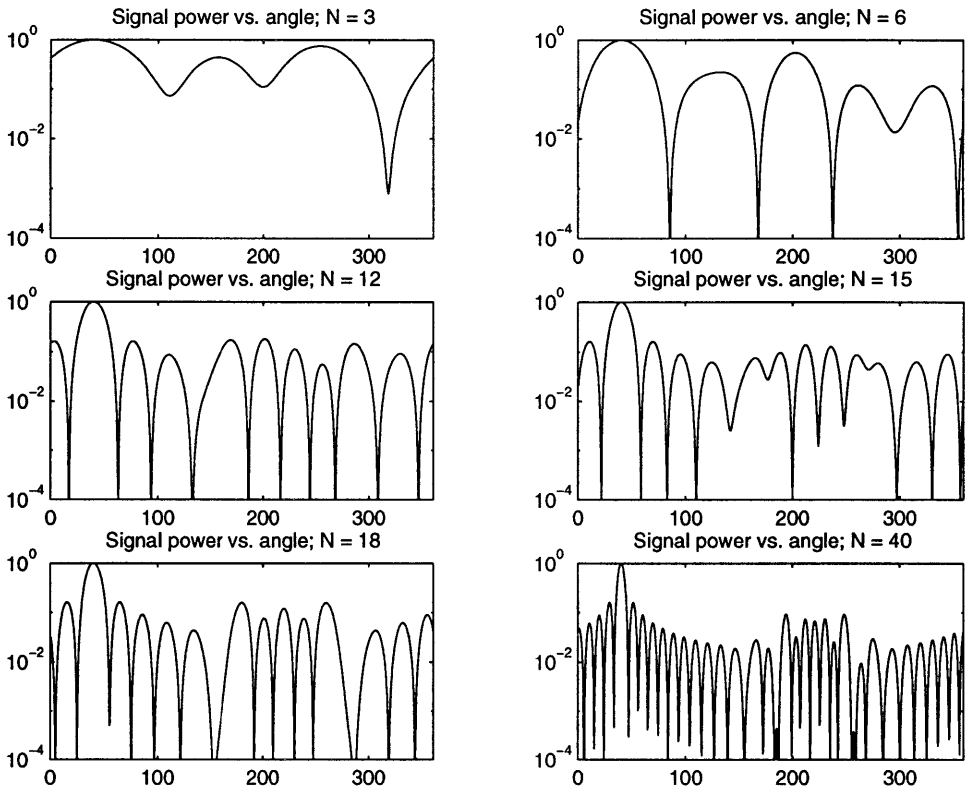

Figure 3.8: Beam pattern as a function of N, the number of elements.

The number of ripples increases with N and that the sidelobe level gradually decreases. However, these sidelobes are generally higher than the sidelobes of linear arrays of equal size. For our system, we choose $N = 12$ as a compromise between array size and directivity.

Chapter 4

CDMA Operation

4.1 CDMA and adaptive antenna arrays

Code Division Multiple Access (CDMA) has proved a reliable and efficient technology for wireless communications [17]. In CDMA systems, all users share the same wideband frequency spectrum. Separation of channels is provided by digital pseudonoise masking codes, which cause each user to appear as white noise to the others. Hence capacity is limited only by the signal-to-noise ratio seen by each mobile. To suppress other-user interference is to increase the capacity (in number of users) and coverage (in area) of each base station.

Our problem, then, is to maximize the signal-to-noise ratio seen by each mobile in both the forward and reverse links. Antenna arrays show great promise in this regard.

Code Division Multiple Access is especially well-suited to a simple implementation of adaptive antenna arrays. Because many users share the same wideband frequency spectrum, a CDMA base station trying to demodulate a user's signal typically faces a multitude (20 or 30) of weak interferers: the other users. It is computationally expensive to track and cancel out each interferer. However, if the users are spread uniformly in space, then we can

steer a beam with the mainlobe oriented towards the the desired user without regard to the location of the other users. With a high probability, many of them will fall outside the mainlobe and be significantly attenuated. We can thus be confident of an increase in signal-to-noise ratio (and consequently capacity) without tracking the location of the interferers. We need only track the desired user.

This is in contrast to narrowband systems,[1] which are characterized by the presence of a few (two to four) strong interferers. For such systems, the interferers must be tracked so that nulls in the beam pattern can be steered towards them. Only then can we ensure a significant degree of interference cancellation.

The following sections describe the basic principles of CDMA operation. We begin with the forward link, in which the BS transmits to the mobile unit.

4.2 Forward link architecture

The base station transmits four types of channels: the *pilot* channel, the *sync* channel, several *paging* channels, and many *traffic* channels. Channel separation is provided by masking each signal by its individual length-64 Walsh code. Walsh codes are mutually orthogonal binary codes. Each user decodes her own transmission by multiplying by her own Walsh code; the orthogonality causes the others to drop out. In the ideal forward link case, then, a user receives zero interference from other users in the same cell.

The pilot channel is used for base station acquisition and to provide a reference for coherent demodulation. A mobile unit constantly seeks BS pilot signals. When it detects one, it sends a request to be added to the new BS's management list. Since the pilot channel is used by all the mobiles and should be easily detectable, it is assigned more power than

[1]The major competing technologies are the analog system AMPS and the digital time division multiple access system GSM. Both are narrowband—each channel takes up only 30 kHz.

the other channels–generally 20% of the total base station broadcast power. The Walsh code used for the pilot channel is W_0, the all-zeros sequence.

The sync channel provides the mobile with timing information to enable synchronization. It is transmitted on W_{32}, the channel of alternating bits.

The paging channels are used to notify sleeping mobiles of incoming calls and to provide overhead information. Typically a base station will have 3 of its 64 channels devoted to paging.

Each mobile is assigned its own traffic channel which carries its voice data. Mobiles currently do not transmit pilot signals because to do so would generate a large amount of interference. However, it has recently been proposed that mobiles transmit pilot signals in the next generation of cellular CDMA. Including pilot signals enables coherent demodulation of the mobile's transmitted signal; it also makes tracking mobiles with antenna arrays substantially easier. For this reason we assume that reverse link pilots are available in this paper.

4.3 Forward link traffic channels

The forward traffic channel generation system can be seen in Figure 4.1. The voice data is first digitally encoded into either a 9.6, 4.8, 2.4, or 1.2 kb/s stream, where the data rate varies with the voice activity. If the data rate is less than 9.6 kb/s, the bits are repeated in order to restore the rate to 9.6 kb/s. The data is then filtered through a rate one-half convolutional encoder to produce a stream at rate 19.2 k symbol/s [17]. (In CDMA, bits are variously referred to as bits, symbols, or chips, depending on their purpose and time duration.) The resulting stream is then block interleaved in frames of length 20 ms.

Meanwhile, the mobile's electronic serial number (ESN) is used to generate a pseudo-

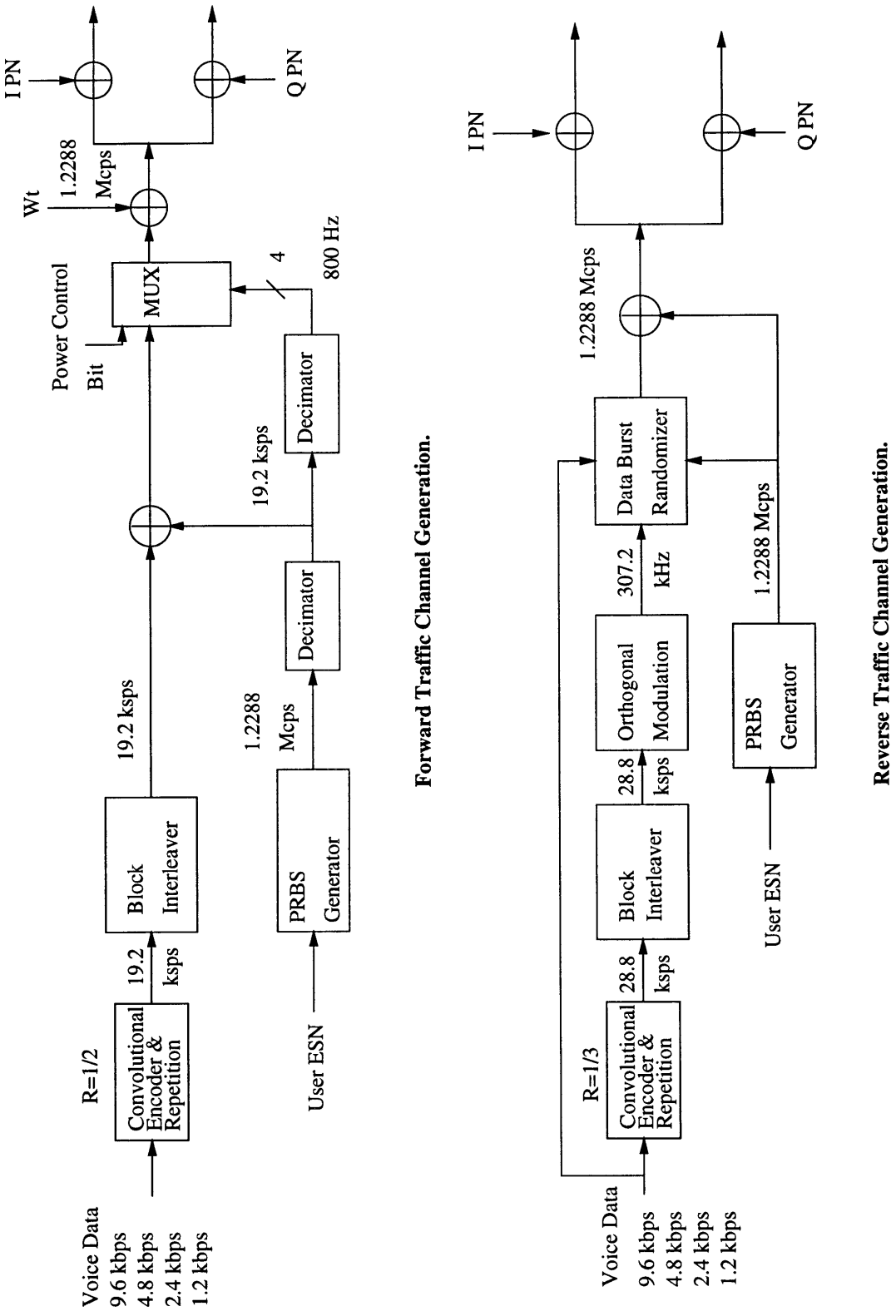

Figure 4.1: Forward and Reverse Traffic Channel Generation.

random bit stream (PRBS) at rate of 1.2288 M chip/s. The chip sequence is decimated to 19.2 k symbol/s and multiplied with the output of the block interleaver in an exclusive-or fashion. This scrambling provides a level of encryption to the user.

The resulting stream is multiplexed with a stream of power control bits which periodically displaces the scrambled data bits. The multiplexed signal, still at 19.2 k symbol/s, is multiplied by the user's Walsh code (at rate 1.2288 Mc/s). The output signal is spread over I and Q quadrature channels (modulated by the BS's pilot sequence) and transmitted. Depending on the original voice activity rate, the stream is broadcast at full, half, quarter, or eighth-rate power.

4.4 Reverse link traffic channels

The reverse link employs no pilot, sync, or paging channels, so our discussion is restricted to the traffic channels. As in the forward link, we begin with digitized voice data encoded at either 9.6, 4.8, 2.4, or 1.2 kb/s. The data is filtered through a rate one-third convolutionally encoder, with repetition at the lower rates to bring the rate back up to 9.6 kb/s. The resulting 28.8 k symbol/s stream is block interleaved at the same rate.

The symbols are transformed into a series of Walsh codes. Each group of six symbols is mapped to the corresponding Walsh code. (Since there are $2^6 = 64$ Walsh codes, we have a perfect correspondence between symbols and Walsh codes.) Note that this is a different use of Walsh codes than on the forward link. There, Walsh codes provided channelization between same-cell users; the code index represented a user channel. Here, Walsh codes spread the signal out in time; a code index represents a symbol sequence.

This sequence and the ESN-generated PRBS are fed into a data burst randomizer. The randomizer removes groups of bits from transmission, so that 4.8 kb/s, 2.4 kb/s, and 1.2

kb/s data rates transmit one-half, one-quarter, and one-eighth of the time, respectively. This approach differs from that of the from the forward link, which transmit continuously at variable rate power rather than transmit at full power at random times. The reason is that tight power control is necessary on the reverse link, and faster power control is possible when transmitting at full power.

The randomizer output is multiplied by the same ESN-generated PRBS and spread over both I and Q quadrature channels for transmission.

4.5 Power control

Since every user appears as interference to the others, it is critical that each user transmit with as little power as possible. Otherwise, mobiles near the BS end up drowning out the transmissions of mobiles near the edges of the cell site. This *near-far* problem is addressed in CDMA through the inclusion of a closed power control loop.

Since shadowing and the fourth-power law are frequency-independent, the mobile uses its received power to estimate the loss over the channel and adjusts its own transmit power accordingly. The adjustment has a relatively slow time constant of 20 ms, since neither shadowing nor path loss changes rapidly with time.

Fast fading varies greatly with frequency, so that the received power at the mobile is not a useful measure of the fast fading for the reverse link. Instead, the mobile adjusts its power up and down in steps of .5 dB according to the power control bits sent by the BS over the traffic channel. The bits arrive 800 times a second; there are thus $1.228 \times 10^6/800 = 1536$ chips per power control bit. Each group of 1536 chips is called a *power control group.*

Chapter 5

Current Research in Smart Antennas

5.1 The forward link

In order to direct a beam towards the mobile, we need to estimate the optimal direction in which to send the signal.

The most obvious method is to estimate the proper direction for forward link transmission from the statistical characteristics of the mobile's reverse link signal. Unfortunately, the frequency separation between forward and reverse links is great enough that the optimal weights for the two links can be significantly different, as demonstrated in Section 2.2.3 [18]. A time-division-duplexing CDMA system, with forward and reverse links alternating transmission on a common frequency, may address this difficulty in the future. At present, however, we cannot rely on the characteristics of the reverse link signal for forward link weight estimation.

The alternative is for the mobile to transmit feedback information to the base station

regarding the quality of the forward link signal. One such proposal, by Akaiwa, uses two dipoles at the base station [1]. During each frame of forward link transmission, one of the two antennas transmits the data; the other antenna is silent. Afterwards, each antenna transmits tones which are known to the mobile, one antenna at a time. The mobile judges between the two tones and informs the base station as to which was better received; the better antenna is used to transmit the following data packet. This design performs best with wide separation between the antenna elements, since it relies not upon beamforming but on independent fading properties.

Liang and Paulraj propose a feedback scheme to mitigate forward link fast fading in an indoor narrowband environment [10]. They periodically perturb the forward link weight vector, observe the resulting perturbation at the mobile, and Kalman filter to estimate the optimal weight vector.

Another issue relevant to antenna array transmission in the forward link is the necessity of the pilot signal. This duality of purpose (phase/timing reference and beacon) complicates forward link design. Each mobile requires a pilot signal that is in phase with its downlink data signal for coherent demodulation; this implies the necessity of multiple beamformed pilots. Mobiles new to the cell site require a pilot that can be acquired from an arbitrary position within the cell site; this implies the necessity of an omnidirectional pilot. To include both a strong omnidirectional pilot and weaker beamformed pilots would seem to consume a prohibitive amount of power. Further research is needed to find the optimal solution.

5.2 The reverse link

The optimal solution to the reverse link problem to maximize some criterion (signal-to-noise ratio, signal energy, etc.) by adjusting the weights of each antenna element without adopting

constraints such as confining one's choices to a particular beam pattern. By adjusting the weights to match the signal's spatial signature exactly, we allow the system to adjust nulls to match clusters of interferers, and peaks to stronger multipath signals. This approach is computationally expensive. Consequently, research has focused on finding a suboptimal, but more computationally tractable, solution to the problem.

Much research has focused on the use of the ESPRIT and MUSIC algorithms for direction-of-arrival (DOA) estimation. These methods require two identical arrays which are separated in space. By calculating the generalized eigenvalues of the covariance matrices of the outputs of these arrays, we can determine the DOA's and an appropriate weight vector. These algorithms require that the number of antennas exceed the number of signals. This is a valid assumption for narrowband wireless technologies. But in CDMA systems, the number of signals generally far exceeds the number of antennas, making use of these algorithms impossible.

A common approach in CDMA is to use a Rake receiver to track multipath elements and beamform towards each element separately, then combine the beamformed signals to yield a single strong signal for processing.

Naguib and Paulraj propose a method for the CDMA case without reverse link pilots [12]. They estimate the array response vector of the desired mobile as the generalized principal eigenvector of a pair of covariance matrices, which provides the optimal set of weights. The first matrix is the covariance of the received signal vector; the second matrix is the covariance of the received signal vector after correlating it with the user's pseudonoise spreading code. They examine the performance of this method by computer simulation and conclude that system capacity increases by a factor equal to the number of antennas per cell site.

Recently a less computationally expensive algorithm for weight vector estimation in cellular CDMA has been proposed [2]. Choi considers the covariance matrix of the array of post-correlated signals. The CDMA correlation process produces a large gain in signal-to-noise ratio, so that it is reasonable to assume that the desired signal power is much greater than the interference power. Under this assumption, he concludes that the eigenvector corresponding to the largest eigenvalue of the post-correlation covariance matrix contains the proper weighting to match the main signal. Since simple algorithms for determining this eigenvector are known, the overall process is computationally simple as well.

Chapter 6

Design Evaluation

The proposed system can be judged according to two metrics: capacity and accuracy in DOA estimation. In this chapter we evaluate each. In Section 6.1, we assume perfect DOA estimation and determine by computer simulation the resulting capacity increase from using a circular adaptive array. In Section 6.2, we consider the probability of accurate estimation both by analysis and by computer simulation.

6.1 Reverse link capacity

We wished to estimate by Matlab simulation the capacity gain from an adaptive beamforming array. We expect that the gain should be approximately equal to the peak-to-average ratio of the antenna pattern, since this is the average amount that interference will be suppressed.

19 cells of equal size were established for the simulation. One cell was placed in the center. This cell was surrounded by two concentric rings. The inner ring was composed of 6 cells; the outer ring was composed of the remaining 12 cells. We randomly placed twenty mobiles inside each cell for a total of 380 mobiles.

The channel characteristics from each mobile to each base station were calculated. The model incorporated both the fourth-power law and lognormal fading ($\sigma = 8$ dB), but not Rayleigh fading. We used the CDMA "best server" rule: each mobile communicates with the base station with which it has the best connection. (This is not necessarily the closest BS to the mobile.) In CDMA optimal power control is such that for any given base station, an equal amount of power is received from each of the mobiles with which it is communicating. Thus, the mobile's transmit power is controlled so that the power is inversely proportional to the strength of its best connection.

Now that all propagation channels and transmit powers have been calculated, it is possible to determine the total power received at the central base station from all 380 mobiles. This quantity is the sum of the product of each mobile's transmit power and the propagation channel between the mobile and the central BS.

This calculation was performed under two hypotheses. In the first hypothesis, each base station had a single omnidirectional antenna, so that the sum is as stated in the previous paragraph. In the second hypothesis, each BS uses an antenna array, so that each mobile's transmission is filtered by the array's beam pattern. (For this hypothesis, perfect DOA estimation was assumed.) The array used is described in [12]; it is a 9-element circular array with radius $\lambda/2$. It has approximate beamwidth 40° with peak sidelobe value .15. Its beam pattern is shown in Figure 6.1.

The simulation was iterated 3000 times to produce Figure 6.2. At top is the cumulative distribution function of the total received interference power at the center BS; below is the probability density function of the received interference. We see that on average the array cuts down interference by about 5.8 dB. This is consistent with the observation that the peak-to-average power ratio of the antenna pattern is about 7.7 dB. The discrepancy is

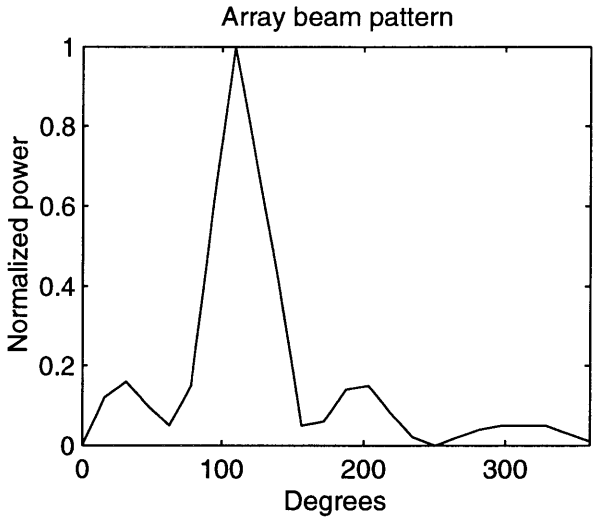

Figure 6.1: Beam pattern used in capacity calculation.

partly due to an imperfection in the random placement algorithm, which does not distribute the MS's perfectly uniformly. This demonstrates the importance of a uniform distribution for beamforming systems; if MS's cluster together, then much of the benefit of beamforming is lost.

A 5.8 dB decrease in interference power is virtually equivalent to a 5.8 dB gain in capacity. This is because in CDMA, each user appears as white noise to all the others. The BS can reliably demodulate each user's signal as long as the signal-to-interference ratio is kept above a certain threshold. If interference power is cut by a factor of 5.8 dB, then the number of users can be multiplied by 5.8 dB while keeping the same interference level. It is thus seen that lowering interference power by a constant factor permits the system to increase capacity by the same factor. (This argument does not take into account the finite availability of Walsh codes for forward link channelization.)

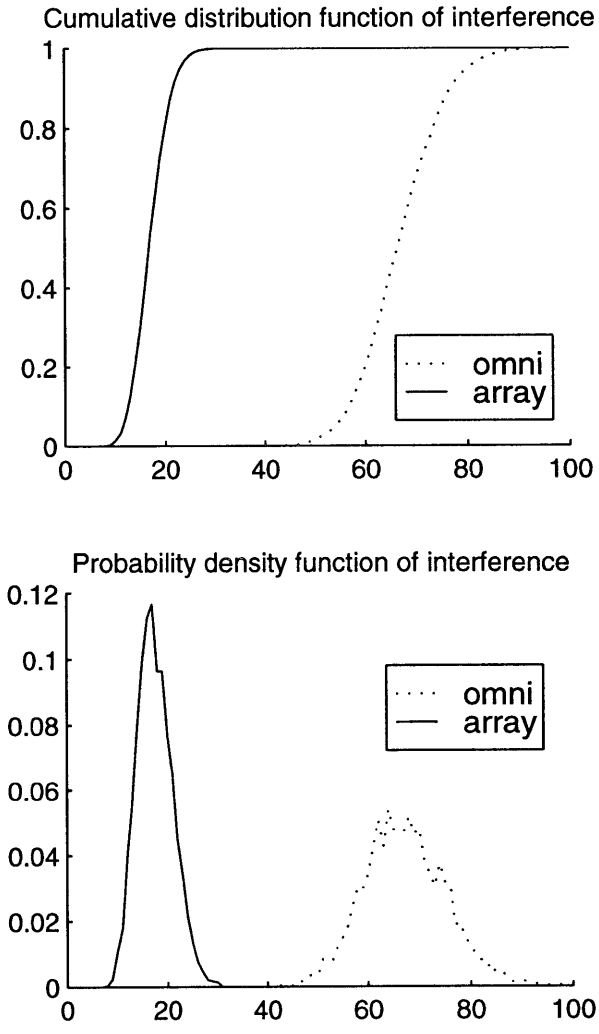

Figure 6.2: CDF and PDF of interference.

6.2 DOA probability of success calculation

6.2.1 Theoretical analysis

We wish to determine the probability that the system estimates the signal DOA to within $\pm 5°$ of the actual DOA. We solve this problem by computer simulation, but first we consider a simpler system for mathematical analysis.

Our system consists of a single base station, a single mobile unit located at direction θ_s, and a single white noise interferer located at direction θ_i. The base station selects between two angles, θ_1 and θ_2, by comparing received energies over a power control group. Our problem is to determine the probability of selecting θ_1 over θ_2.

The pilot signal, despread and integrated over the power control group, is $1 + j$; the interferer signal is $I(u + jv)$, where u, v are independent Gaussian random variables with zero mean and unit variance, and I is the square root of the ratio of the interference power to the signal power. Let G be the gain seen by the user under hypothesis θ_1; B be his gain for θ_2, and H and C be the gains of the interferer for θ_1 and θ_2 respectively. We assume without loss of generality that $|G| > |B|$; that is, θ_1 is a better fit to θ_s than θ_2 is.

We restrict our attention to the case where the gains are all real. This holds for our implementation of circular arrays when the number of antenna elements is even.

The received signals under hypotheses θ_1 and θ_2 after CDMA correlation and time integration are

$$\text{Signal}(\theta_1) = (1 + j)G + I(u + jv)H = (G + IHu) + j(G + IHv) \tag{6.1}$$

$$\text{Signal}(\theta_2) = (1 + j)B + I(u + jv)C = (B + ICu) + j(B + ICv) \tag{6.2}$$

We wish to calculate the energy received under each hypothesis. Taking the difference of the squares of the magnitudes of each, we obtain

$$\mathrm{En}(\theta_1) - \mathrm{En}(\theta_2) = I^2(H^2 - C^2)(u^2 + v^2) + 2I(GH - BC)(u + v) + 2(G^2 - B^2) \quad (6.3)$$

If this quantity is positive, the BS will select θ_1. If it is negative, the BS will select θ_2.

To simplify the discussion, we define

$$M = I\sqrt{|C^2 - H^2|}; \quad N = \frac{HG - CB}{\sqrt{|C^2 - H^2|}} \quad (6.4)$$

We divide the possibilities into two cases: $|C| > |H|$ and $|C| < |H|$. (If $|C| = |H|$, then our system will choose hypothesis θ_1 with probability 1, since we stipulated that $|G| > |B|$.) If $|C| > |H|$, the interfering signal is stronger in the θ_2 direction. If $|C| < |H|$, the interferer is stronger in the θ_1 direction.

Case 1: $|C| > |H|$. In this case, we complete the square in u and v as follows:

$$\mathrm{En}(\theta_1) - \mathrm{En}(\theta_2) = -(Mu + N)^2 - (Mv + N)^2 + 2N^2 + 2(G^2 - B^2) \quad (6.5)$$

Case 2: $|H| > |C|$. We obtain, similarly,

$$\mathrm{En}(\theta_1) - \mathrm{En}(\theta_2) = -(Mu + N)^2 - (Mv + N)^2 - 2N^2 + 2(G^2 - B^2) \quad (6.6)$$

In either case, the quantities in the form $p = Mu + N$ and $q = Mv + N$ are independent Gaussian random variables with mean N and $\sigma^2 = M^2$.

We can now determine the probability of selecting θ_1. For case 1,

$$P[\text{Energy}(\theta_1) - \text{Energy}(\theta_2) > 0] = \frac{1}{2\pi M^2} \iint_O \exp(-\frac{p^2+q^2}{2\sigma^2}) dpdq \tag{6.7}$$

where O is the circle centered about the origin in the $p-q$ plane with radius

$$R = \sqrt{N^2 + 2(G^2 - B^2)} \tag{6.8}$$

For case 2, if

$$-2N^2 + 2(G^2 - B^2) \geq 0 \tag{6.9}$$

then the probability of selecting θ_1 is unity. Otherwise, the probability is

$$P[\text{En}(\theta_1) - \text{En}(\theta_2) > 0] = 1 - \frac{1}{2\pi M^2} \iint_O \exp(-\frac{p^2+q^2}{2\sigma^2}) dpdq \tag{6.10}$$

where the region of integration is the same circle as in Case 1.

We divide p and q by $M\sqrt{2}$ to obtain p' and q', random variables with mean $N/(M\sqrt{2})$ and $\sigma^2 = .5$. Since p and q are independent, p' and q' are independent also. We calculate the joint distribution of p' and q'.

$$p_{p',q'}(P', Q') = \frac{1}{\pi} \exp\left(P'^2 + Q'^2\right) \tag{6.11}$$

We define

$$\text{SNR} = \frac{(HG - CB)^2}{I^2(C^2 - H^2)^2} = N^2/I^2 \tag{6.12}$$

and

$$r = \sqrt{p'^2 + q'^2}; \quad \theta = \arctan(q'/p') \tag{6.13}$$

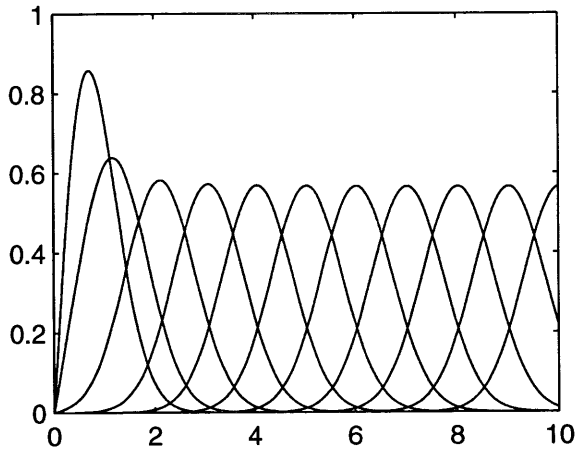

Figure 6.3: Rice probability distribution functions for SNR=0, 1, 4, 9... 100.

where arctan is a 2π-arctangent, since we know the signs of p' and q'. Now we have

$$p_{r,\theta}(R,\Theta) = p_{x,y}(R\cos\Theta, R\sin\Theta)R \tag{6.14}$$

$$= \frac{R}{\pi}\exp\left[-\left(R\cos\Theta - \sqrt{.5\mathrm{SNR}}\right)^2 - \left(R\sin\Theta - \sqrt{.5\mathrm{SNR}}\right)^2\right] \tag{6.15}$$

$$= \frac{R}{\pi}\exp[-R^2 + R\sqrt{2\mathrm{SNR}}(\sin\Theta + \cos\Theta) - \mathrm{SNR}] \tag{6.16}$$

Hence, integrating from 0 to 2π with respect to θ, we obtain

$$p_r(R) = 2R\exp(-R^2 - \mathrm{SNR})[I_0(2R\sqrt{\mathrm{SNR}})] \tag{6.17}$$

where I_0 is the zeroth-order modified Bessel function of the first kind. r has the Rice distribution, which is plotted in Figure 6.3 for several different values of SNR. Its CDF is shown in Figure 6.4.

We also note a special case. If $\theta_1 = \theta_s$, $\theta_2 = \theta_i$, and the array is symmetric, then $G = C$ and $H = B$, and p and q both have zero mean. (Since $\theta_2 = \theta_i$, this falls under Case 2.) In

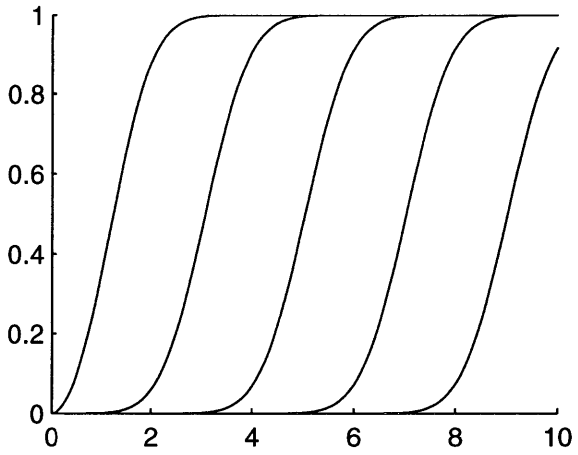

Figure 6.4: Rice cumulative distribution function for SNR=1, 9, 25,49, 81.

this case, SNR = 0, and $I_0(2R\sqrt{\text{SNR}}) = I_0(0) = 1$. Then, integrating Equation 6.17,

$$P(r < R) = \int_0^R 2r \exp(-r^2) dr = 1 - \exp(-R^2) \tag{6.18}$$

For our decision rule, we choose R as in Equation 6.8. For one power control group in IS-95A CDMA, $I^2 = -11$ dB. This results in a probability of success of 97%, independent of the particular values of G, C, H, and B.

6.2.2 Computer simulation

Matlab was used to estimate the capacity of a BS equipped with the adaptive array system.

We placed a single BS in the $x - y$ plane. Multi-user interference was simulated by uniformly distributing 16 interferers about the unit circle. Each interferer was chosen to have equal average power. At each power control group (duration 1.25 ms), a complex random variable with independent Gaussian real and imaginary parts was assigned to each user to represent its transmission power. (Since each user's signal is masked by a pseudorandom bit sequence, it is reasonable to treat each interferer as white Gaussian noise.) These random

variables were processed by the beam pattern of the array and added to the signal of the desired user. Then, after each power control group, the energies were calculated under a variety of hypotheses: $0°, 10°, 20°, ...350°$. The angle which resulted in the maximum energy was used for processing.

The maximum energy was used for power control. If the received energy was greater than a threshold γ, the MS decreased its transmission power by .5 dB. If the energy was less than γ, the MS increased its transmssion power by .5 dB. γ was chosen so that, on the average,

$$\frac{E_c}{I_0} = -21\text{dB} \Longrightarrow \frac{E_{\text{pcg}}}{I_0} = 11\text{dB} \tag{6.19}$$

where E_c is the signal energy per chip, E_{pcg} denotes the energy per power control group (1536 chips), and I_0 is the interference energy.

An approximation to Rayleigh fading was generated [7]. First each of two independent Gaussian white noise sources is put through a low-pass filter. The first and second sources are modulated by $\cos\omega t$ and $\sin\omega t$ respectively. The sum of the outputs is then multiplied by the mobile's transmission to obtain the received signal at the BS. This method provides uniform phase modulation and Rayleigh envelope fading as desired. The result is shown in Figure 2.2.

Essentially, we modeled the calculation

$$\text{Energy}(\theta_i) = \left| \sum_{k=1}^{K} e^{j\phi_{k,i}} \int_0^T x_k(t)c(t)dt \right|^2 \tag{6.20}$$

where K is the number of array elements, k is the element index, $\phi_{k,i}$ is the assigned phase for antenna k for angle θ_i, $x_k(t)$ is the signal received at antenna k, $c(t)$ is the desired user's pseudorandom bit stream, and T is the period of integration (here one power control group,

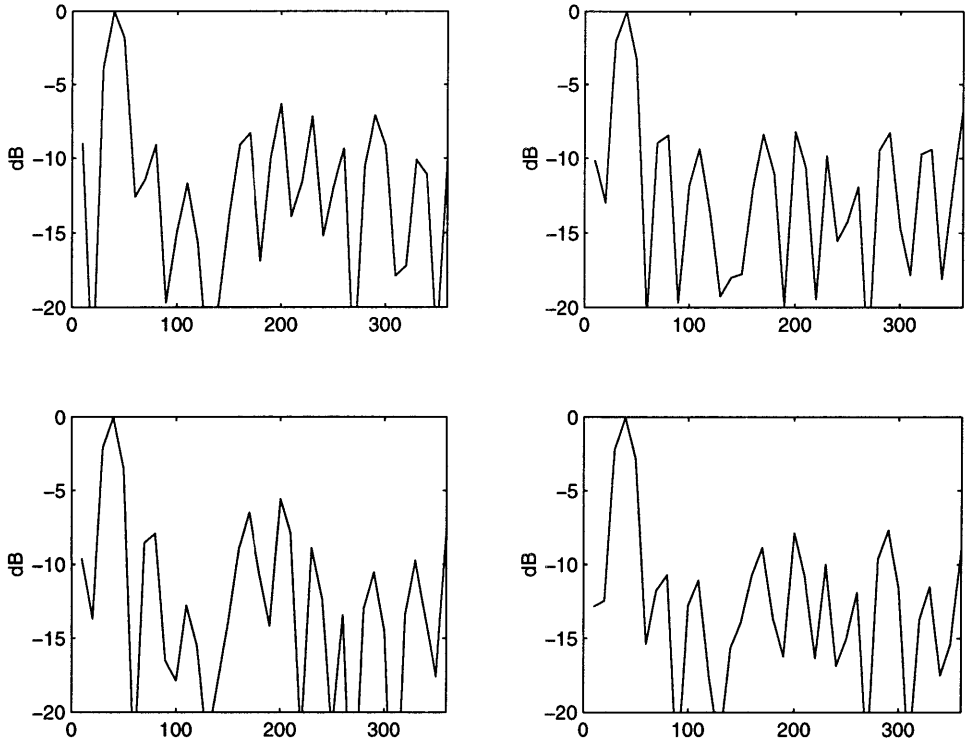

Figure 6.5: Energies received under various angle hypotheses.

or 1536 chips). (The difference between the simulation and reality is that the simulation used a single random variable to model the energy over the power control group rather than calculate the pseudorandom bit sequence $c(t)$.) We then compared all these energies and selected the angle associated with the maximum energy to return as our estimate.

We assumed that power control would mitigate slow fading, so that it was not considered in the simulation. Figure 6.5 shows received energy patterns for the case without fast fading (equivalently, perfect power control). The patterns show a maximum at 40°, the position of the desired user. As expected, these patterns are similar to system beam pattern (shown in Figure 3.8 for $N = 12$).

For the case with fast fading, we ran a simulation that lasted for 200 power control groups (.25 s). At each power control group, the angle yielding maximum energy was noted. The

user location	10	20	30	40	50	other
30	0	0	.96	.01	0	.03
31	0	.005	.96	.015	0	.02
32	0	0	.95	.03	0	.015
33	.005	0	.915	.075	0	.005
34	0	0	.79	.18	0	.03
35	0	0	.54	.46	0	0
36	0	.005	.16	.83	0	.005
37	0	0	.075	.915	.005	.005
38	0	0	.015	.98	0	.05
39	0	0	.005	.995	0	0
40	0	0	0	.965	0	.035

Figure 6.6: Frequencies of occurrence with fast fading. The true DOA of the user is shown in the left-hand column. At right is the relative probability that each of the angles 10°, 20°, ... 50° were chosen as the DOA estimate.

simulation was run eleven times; for each time, the user was located at a different angle in the interval (30°, 40°). The frequencies of occurrence are shown in Figure 6.2.2.

The probability that the estimate is within ±5° of the true DOA is quite high. In the least favorable case, when the MS is located halfway between 30° and 40°, either estimate is about equally likely. We also observe that when the estimator fails to choose the best estimate, it often returns an angle differing from the optimal estimate by ±10°. Even this suboptimal result yields a useful degree of interference suppression and SNR gain.

Chapter 7

Conclusions

This project examined the possibility of using adaptive antenna arrays in conjunction with CDMA base stations. We demonstrated that a beamforming 12-element array can increase capacity by 5.8 dB, assuming perfect DOA estimation. Mathematical analysis and computer simulation indicate that the simple DOA estimator can achieve reasonable levels of accuracy.

This performance is contingent upon the assumption that the BS is located in a remote location without local scatterers. If this is not the case, then a diversity array or microcell would be more effective.

The use of smart antennas in wireless mobile communications is an extremely active area of investigation. The most promising approach is to determine the optimal weight vector [12] by eigenvector estimation. It is hoped that further developments in signal processing technology will make such approaches viable for commercial use in the near future.

Bibliography

[1] Y. Akaiwa. "Antenna selection diversity for framed digital signal transmission in mobile radio channel." In *Proc. VTC '89,* vol. I, pp.85-88, Nov. 1993.

[2] S. Choi, "Design of an adaptive antenna array for tracking the source of maximum power and its application to CDMA mobile communications," *IEEE Trans. on Antennas and Propagation,* 45(9), Sept. 1997.

[3] *EMS Wireless Product Catalog,* September 1997.

[4] R. C. French, "The effect of fading and shadowing on channel reuse in mobile radio," *IEEE Trans. Veh. Technol.,* vol. 39, no. 1, pp. 56-67, Feb. 1990.

[5] L. Godara. "Applications of antenna arrays to mobile communications, part I: Performance improvement, feasibility, and system considerations," *Proc. of the IEEE,* 85(7), pp. 1031-1060, July 1997.

[6] G. Golden and J. Winters. "Adaptive antenna array applique field test." Presented at the Fourth Workshop on Smart Antennas in Wireless Mobile Communications, Stanford University, July 1997.

[7] W. C. Jakes, *Microwave Mobile Communications.* New York, NY: IEEE Press, 1974.

[8] J. A. Kong, *Electromagnetic Wave Theory, Second Edition.* New York, NY: John Wiley & Sons, 1990.

[9] W. C. Y. Lee. "Angle spread versus base station antenna heights." Presented at the Fourth Workshop on Smart Antennas in Wireless Mobile Communications, Stanford, CA, July 1997.

[10] J. W. Liang and A. Paulraj. "Forward link antenna diversity using feedback for indoor communication systems." In *ICASSP-95 Conference,* Detroit, MI, 1995.

[11] M. T. Ma, *Theory and Application of Antenna Arrays.* New York, NY: John Wiley & Sons, 1974.

[12] A. F. Naguib and A. Paulraj. "Performance of wireless CDMA with M-ary orthogonal modulation and cell site antenna arrays." *IEEE Journal on Selected Areas in Communications,* 14(9):1770-1783, Dec. 1996.

[13] Y. Nomura, "On the diffraction of electromagnetic waves by a perfectly reflecting wedge," Res. Inst. Tohoku University, Japan, Scientific Repts., Series B, vol. 1 and 2, No. 1, pp. 1-24; 1951.

[14] Y. Ohba, "On the radiation pattern of a corner reflector finite in width." *IEEE Transactions on Antennas and Propagation,* 127-132, March 1963.

[15] Y. Ohba, "Directional characteristics of a dipole antenna with a rectangular reflector," *Journal of Applied Physics* (Japan), vol. 26, pp. 11-17; January 1957.

[16] R. Steele, *Mobile Radio Communications.* New York, NY: IEEE Press, 1992.

[17] A. J. Viterbi, *Principles of Spread Spectrum Multiple Access Communications.* Reading, MA: Addison-Wesley, 1995.

[18] J. H. Winters, "Signal acquisition and tracking with adaptive arrays in wireless systems," in *Proc. 43rd Veh. Technol. Conf.*, vol. I, pp. 85-88, Nov. 1993.